RSC Advances

ROYAL SOCIETY OF CHEMISTRY

www.rsc.org/advances

RSC Advances RSCPublishing

ARTICLE

Degradation of Tetracycline Hydrochloride by Heterogeneous Fenton-like reaction using Fe@ *Bacillus Subtilis*

Cite this: DOI: 10.1039/x0xx00000x

Pei Zheng [a], Bo Bai [*, b], Weisheng Guan [a], Honglun Wang [b], Yourui Suo [b]

Received 00th January 2012,
Accepted 00th January 2012

DOI: 10.1039/x0xx00000x

www.rsc.org/

A novel heterogeneous catalyst Fe@ *Bacillus subtilis* has been synthesized though the impregnation method with Iron (III) chloride hexahydrate. Field emission scanning electron microscopy (FE-SEM), energy dispersive spectrometry (EDS), energy dispersive X-ray (EDX) mapping, X-ray photoelectron spectroscopy (XPS) and Fourier transform infrared spectroscopy (FT-IR) were used to characterize the materials. The as-prepared materials were employed as a heterogeneous Fenton's reagent with the addition of H_2O_2 for degradation of Tetracycline Hydrochloride (TC). This new heterogeneous Fenton-like system resulted in a nearly total elimination of TC and a negligible release of iron leaching from the catalyst was achieved. The catalytic performance could be maintained in three consecutive runs without a significant drop. This behavior was attributed to the synergistic structural and functional effect of the combined *B. subtilis* and iron ions. The FTIR and XPS characterizations of the catalyst before and after Fenton-like reaction showed that the no structural deformation of the particles was occurred.

Introduction

Antibiotics, comprising a significant amount of pharmaceutical compounds, are widely used in concentrated animal feeding operations around the world to treat the diseases and improve the growth rate of animals [1, 2]. However, the majority of antibiotics are excreted in forms of feces and urine without digestion and metabolism by animals [3]. The large number of antibiotic residues leads to the emergence of environmental issues, such as the threat to aquatic life, indigenous microbial populations and the risk posed by antibiotic-resistant pathogens etc. [4]. Thus, it is of great significance to develop efficient and cost-effective technologies to remove antibiotics from aquatic environment. In practice, the antibiotics residues are hard to be treated by the traditional methods such as physical adsorption and biological degradation due to its antibacterial nature and the difficulty faced on the post-treatment of sorbents [5].

The Advanced Oxidation Processes (AOPs), as a promising method, have presented the predominance to remove the recalcitrant and non-biodegradable compounds through the generation of highly reactive radicals (e.g. hydroxyl free radicals) [6]. In particular, homogeneous Fenton (H_2O_2/Fe^{2+}) and Fenton-like (H_2O_2/Fe^{3+}) systems-which are based on ferrous ion and hydrogen peroxide-are proven to be effective technologies for destruction of a large number of hazardous and organic pollutants [7-10]. It may also be operated at or near room temperature and atmospheric pressure [8]. Moreover, the oxidant used (hydrogen peroxide) breaks down into environmental friendly species like water and oxygen [9]. However, some significant disadvantages, such as narrow pH range required, the production of iron-containing waste sludge, and high concentration of iron needed for successful mineralization which introduces secondary pollution, impede the large scale application of such technologies at the industrial level [10, 11]. In order to overcome these disadvantages, much effort has been made to develop heterogeneous Fenton-like catalysts such as iron-containing mesoporous materials with similar catalytic activities as homogeneous Fenton system [12-16]. Fe-ions have been reported to be immobilized by support materials like membrane [12], C-fabrics [13], zeolite [14], clays [15] and montmorillonite [16].

Recently, microbial cells as support materials have attracted burgeoning interests due to the major advantages, including abundant resources, easy accessibility, renewable and environmentally friendly and easy to remove [17]. *Bacillus subtilis*, known as a member of the genus Bacillus, is an extremely common bacterium found in soil, water, air,

and decomposing plant matter [18]. Due to its abundant resources and special physicochemical/biological properties, *B. subtilis* exhibits an ideal candidate as a microbial cell template for the formation of micro-nano photocatalytic composite materials [19]. Specifically, *B. subtilis* cells has a rigid and peritrichous structure cell wall which comprised virtually of 46 % peptidoglycan and 54 % teichoic acids and is abundant in functional groups like hydroxyl, acylamino, carboxyl and amino groups [20]. Therefore, such coexistence of peritrichous structure and the hydrophilic functional groups in the framework of *B. subtilis* cell wall provides plentiful absorption sites and excellent absorbability, which makes a good reason to utilize *B. subtilis* as a support to synthesize micro-nano photocatalytic composite materials [17, 21]. However, no one has reported the synthesis of Fe-catalyst materials with *B. subtilis* cells as support material. Therefore, based on what has been illustrated above, we firstly present a Fe@ *B. subtilis* composite material loaded with Fe-ions as an immobilized catalyst being applied to decompose antibiotics by Fenton-like reactions. The as-prepared Fe@ *B. subtilis* samples were characterized using FE-SEM, EDS, EDX, FT-IR and XPS, respectively. Tetracycline hydrochloride (TC) was selected as an object pollutant to examine the catalytic performances of the designed Fe@ *B. subtilis* catalyst.

Experimental

Materials preparation

In our works, Fe@*B. subtilis* composite was firstly synthesized through the impregnation method using Iron (III) chloride hexahydrate ($FeCl_3 \cdot 6H_2O$) as a single iron source and *B. subtilis* as support of the active phase. Briefly, 1.000 g of *B. subtilis* powder was washed with distilled water and ethanol for three times. Then, the washed *B. subtilis* was wet impregnated at room temperature using 50 mL saturated iron chloride solution as precursor with the help of magnetic stirring for 1h. After that, the above mixture was left for 24.0 h at ambient temperature and pressure to form the Fe@ *B. subtilis* composite. The resulting particles were collected by centrifugation from the mixture, followed by two cycles of distilled water rinsing. The obtained Fe@ *B. subtilis* particles were dried in air at 50 ^{o}C for 6 h and stored in a sealed bottle for further use.

Materials characterization

Several techniques were used to characterize the composite microspheres. After sputtering Pt onto the samples, the morphology of the sample was examined by fieldemission scanning electromicroscopy (FE-SEM, JEOL-6300F). A detailed composition characterization was carried out by energy dispersive spectroscopy (EDS) analysis and energy dispersive X-ray (EDX) mapping. Fourier-transform infrared (FT-IR) spectra of samples were recorded on a Bio-Rad FTS135 spectrometer in the range 400-4000 cm^{-1} using a KBr wafer technique. X-ray diffraction (XRD) patterns were conducted on X. Pert Pro diffractometer using Cu Kα radiation (λ = 0.15418 nm) at a scanning rate of 10°per min to investigate the crystal structures and the phase compositions of the samples. The X-ray photoelectron spectroscopy (XPS) spectra were obtained with an ESCALab220i-XL electron spectrometer (VG Scientific) using 300 W Al-Ka radiation.

Catalytic performance

Catalytic experiments were performed in a batch glass reactor with semi-batch operation mode, at atmospheric pressure and ambient temperature, under continuous stirring. In a typical run, the samples were introduced into the reactor, loading with 100 mL 25 mg L^{-1} of TC solution, with magnetic stirring to maintain a uniform suspension. After allowing 160 min for the adsorption/desorption of TC to reach equilibrium, 2 mL H_2O_2 (30%) was added into the reactor and time logged. Samplings were taken at regular intervals during the reaction and analyzed immediately after centrifugation to remove suspended particles. A UV–vis Spectrophotometer ((UV-752, Shanghai)) was used to follow the TC concentration histories, i.e., concentration evolution along reaction time, at λ_{max}= 356 nm.

In this work, the effect of hydrogen peroxide dose to TC degradation has also been investigated and experiments were conducted, applying an aqueous TC solution (100 mL in volume containing 30 mg L^{-1} of TC). The catalyst and H_2O_2 were added to the reaction system at the start of each run.

Stability and reusability

To test the stability and reusability of the Fe@ *B. subtilis* catalyst, three runs were conducted with the same reaction conditions. The used Fe@ *B. subtilis* catalyst was removed, and then washed before each runs. Meanwhile, the conversions of TC as well as iron leaching concentration in the solution were monitored.

Settling performance

At room temperature 50.0 mg Fe@ *B. subtilis* samples, *B. subtilis* and Iron chloride hexahydrate were dispersed into 50 mL of distilled water without any additional addictive in a vertical cylindrical burette, respectively. The falling height was determined at regular time intervals. The sedimentation ratio (SR) was measured by:

$$SR = \frac{a}{a+b} \times 100\% \quad (1)$$

a is the length of the clear fluid and b the length of the turbid fluid, respectively.

Results and discussion

Characterization

Figure 1shows the SEM images of the naked *B. subtilis* and Fe@ *B. subtilis* composite particles. In Figure 1a and b, the primitive *B. subtilis* cells were ordered rod-shaped with the

length of approximately 1.4 ± 0.2 μm and width of 0.6 ± 0.1μm (Figure S1). From Figure 1c and d, the Fe@ *B. subtilis* composite particles maintained the shape of the primitive *B. subtilis* cores and possessed relatively better monodispersity. The insert images in Figure 1b and 1d presented the EDS analysis of *B. subtilis* and Fe@ B. subtilis composite particles. The detection of Fe element (the insert image in Figure 1d) obviously provided an evidence of the existence of iron ions on the surface of the *B. subtilis* cells. By comparing the weight concentration of C, N, O, S, Cl and Fe in Table 1(Table S1), the C, N, O and S weight concentration in the Fe@ *B. subtilis* decreased, which might be attributed to the attachment of ferric trichloride onto the surfaces of *B. subtilis*.

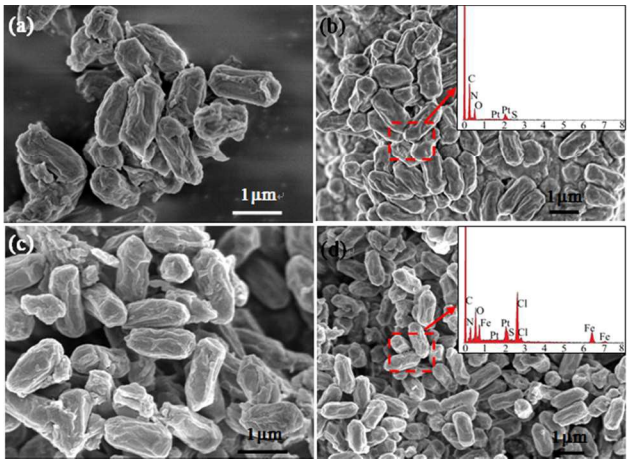

Fig. 1 SEM images and EDS spectrum of naked *B. subtilis* (a, b) and Fe@*B. subtilis* (c, d).

The homogeneity of chemical composition was investigated by two-dimensional X-ray mapping of selected Fe@ *B. subtilis* zones (Figure 2). The clear C, O and Fe elemental mapping images of Fe@ *B. subtilis* in Figure 2(b-d) indicated the homogeneous dispersions of C, O, and Fe elements on the surface of *B. subtilis* support. Moreover, the elaborative observation of Figure 2d confirmed that iron ions were almost uniformly deposited on the *B. subtilis* surface.

Figure 3 exhibited the FT-IR spectra of original *B. subtilis*, and Fe@ *B. subtilis* composite particles. For *B. subtilis*, the broad and intense peak located at about 3410 cm^{-1} could be assignable to the -OH stretching vibration. The peaks of amide groups in *B. subtilis* protein can be observed at 1650 $cm^{-1}$and 1542 cm^{-1} [22]. The adsorption bands around 2924 and 2852 cm^{-1} can be attributed to the $-CH_2-$ asymmetric and symmetric stretching. In addition, the characteristic bands at 1070 cm^{-1}, 1230 and 1382 were assigned to the stretching vibration of C-O group, C-O-C vibration in cyclic ether moieties and O-H vibration in carboxyl acid, respectively [23-25]. As for Fe@ *B. subtilis* in Figure 3a, the characteristic absorption peaks at 3400, 2924, 2852, 1650, 1542, 1382, 1230 cm^{-1} decreased and shifted dramaticly, compared with the spectrum of original *B. subtilis*, implying that the functional groups on the *B. subtilis* have some kind of interaction with the iron ions.

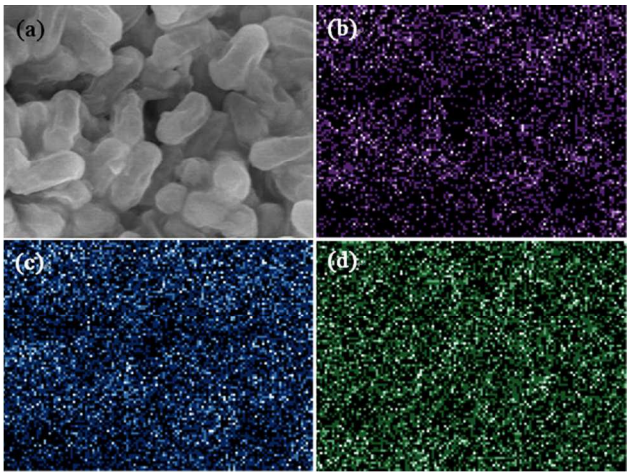

Fig. 2 Selected zones of Fe@*B. subtilis* samples (a) and corresponding X-ray mapping, (b) for C, (c) O, and (d) Fe elements.

XRD spectra of the bare B. subtilis and Fe@Bacillus subtilis composite particles were exhibited in Fig. 3b. As depicted Fig. 3b, the broad peak around $2\theta=20^{o}$ was attributed to the amorphous phase of B. subtilis. After anchoring the iron ions on the Bacillus subtilis, the broad peak almost disappear. The surface element compositions and the valence states of the Fe@ *B. subtilis* catalyst were revealed by XPS. Figure 3c shows the fully scanned spectra in the range of 200-800 eV. As seen in Figure 3c, the wide scan spectra of the Fe@*B. subtilis* exhibited photoelectron lines at binding energies of ~200, 285, 399, 530 and 711 eV which are ascribed to Cl 2p, C 1s, N 1s, O 1s and Fe2p, respectively. The binding energy peaks at 710.9 and 724.5 eV in the high resolution Fe 2p scan (Figure 3d) correspond to Fe 2p3/2 and Fe 2p1/2, respectively [26]. The peak (719.1 eV) located approximately 8 eV higher than the main Fe 2p3/2 peak was the satellite peak of Fe 2p3/2, indicating the ionic state of Fe^{3+} [27, 28]. Moreover, the elemental concentration in atomic % (at. %) of C, N, O, Cl and Fe determined by relative sensitivity factors (RSFs) and the spectra intensities were 76.4, 1.88, 16.7, 2.86 and 2.24 %, respectively (Table S2).

The results obtained by N_2 adsorption/desorption measurement (77 K) for Bacillus subtilis and Fe@B. subtilis are depicted in Fig. 4. All the isotherms exhibited a type IV pattern according to the International Union of Pure and Applied Chemistry (IUPAC) classification, which corresponds to mesoporous materials, and this can also be affirmed by the pore size distribution (Fig. 4 inset). Their textural properties such as surface area, pore size are summarized in Table S3. The surface areas for Bacillus subtilis and Fe@ B. subtilis were 4.94 and 6.95 m^2 g^{-1}, respectively. The Barrett-Joyner-Halenda (BJH) pore size distribution (Fig.4 inset, using the desorption branches) analyses revealed that the average pore sizes of Bacillus subtilis and Fe@B. subtilis were 5.9 and 6.1 nm, respectively, and were in the mesoporous range of 2-50 nm according to the IUPAC classification [29, 30].

Settling test

The sedimentation performance of Fe@ *B. subtilis* in aqueous solutions was also evaluated to demonstrate the unique features of Fe@ *B. subtilis* in comparison with *B. subtilis* and iron ions. It can be clearly observed in Fig. 5 that the suspension ability of Fe@ *B. subtilis* (56 %) is better than *B. subtilis* (13%) and iron ions (nearly zero). It was also observed in the experimental process that slight agitation or vibration could make the settled Fe@ *B. subtilis* re-suspend in aqueous solution. Therefore, in practical applications, lower stirring speeds may ensure the full contact between the Fe@ *B. subtilis* and the contaminants. Moreover, one of the main merits of applying heterogeneous catalyst is to promote the separation operation. Thus, the relatively large particles in suspensions can allow easy separation and reuse of the catalyst.

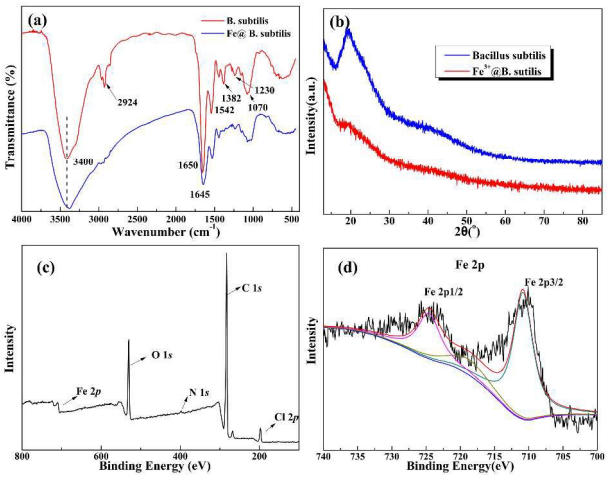

Fig.3 (a) FT-IR spectra and (b) XRD patterns of *B. subtilis* and Fe@*B. subtilis;* (c) wide scan XPS spectra and (d) high resolution Fe 2p spectra of Fe@ *B. subtilis*.

Catalytic performance

Fenton-like reaction based on ferric ions and H_2O_2 has been reported as an effective method to degrade organic pollutants by oxidation in aqueous solutions. Iron-containing materials are commonly used as catalysts for Fenton-like reactions and have shown relatively high activities [13, 15, 31]. In this study, Fenton-like reactions were carried out for tetracycline hydrochloride degradation, the antibiotic second highest in production and use, to test the activities of the prepared Fe@*B. subtilis*. No acid or base solutions were used to adjust the pH value of the reaction system and all experiments were carried out in the dark to avoid the effect of light.

As shown in Fig. 6, before the addition of H_2O_2, the self-degradation of the tetracycline hydrochloride is negligible and so did iron ions. *B. subtilis* and Fe@B. subtilis showed certain ability to remove nearly 36.0 and 46.8 % of tetracycline hydrochloride concentration due to the synthetic effect of textural properties, surface functional groups and electrostatic attraction. Firstly, based on the FT-IR spectrum, the proved surface functional groups on the Bacillus subtilis and Fe@ B. subtilis may bond with the tetracycline hydrochloride molecules. Secondly, the experimental pH (~6.0) was between the pKa1 (3.3) and pKa2 (7.7) of tetracycline hydrochloride. At this pH value, TC would be partially in its cationic form, which is important for the electrostatic attraction since both Bacillus subtilis and Fe@B. subtilis showed negatively charge at this pH value (as illustrated in Fig. S2). In the presence of 2 mL of H_2O_2, the oxidation of tetracycline hydrochloride in parallel system was still negligible, whereas the iron ions system exhibited certain ability to decrease the tetracycline hydrochloride concentration during the first 30 min, as nearly 44% concentration decrease was observed. However, the concentration of tetracycline hydrochloride remained almost unchanged from then on, indicating that the concentration decrease was due to the Fenton-like oxidation of tetracycline hydrochloride molecules initiate by ferric ions. This phenomenon also demonstrated that the oxidation ability in the iron ions system can only maintain a short time and thus showed a restricted application.

Moreover, nearly 93.5% of tetracycline hydrochloride was removed by Fe@ *B. subtilis*. The great progress happened to Fe@ *B. subtilis* compared to bare *B. subtilis* and iron ions can be attributed to the integration of adsorption by the *B. subtilis* bodies with Fenton-like oxidation by the ferric ions attached on the *B. subtilis* surface. Specifically, *B. subtilis* can adsorb the TC molecules from the bulk solution and enrich them on the surface of the catalyst, resulting in a higher reactant concentration, which was similar to the role of mesoporous SiO_2 shell reported by Cui et al. [32]. Moreover, the removal of TC via adsorption of the *B. subtilis* surface is preserved by keeping the adsorption sites unsaturated through the decomposition of the molecules by Fe^{3+}/H_2O_2 Fenton-like system, which increases the active sites for generation of hydroxyl (HO·) and perhydroxy (HOO·). Li et al. have investigated the radical intermediates involved in the Fenton reaction system by using radical scavengers [33]. Their experiment indicated that hydroxyl (HO·) and perhydroxy (HOO·) radicals are active radical intermediates involved in the reaction, but they are not the only species. The singlet oxygen $^1O_2$ produced from HOO· and HO· is directly participated in the degradation of organics. Thus, the relevant radical reactions can be proposed as shown in Eqs. (2)-(9) [33, 34].

$$Fe^{III} + H_2O_2 \rightarrow Fe^{II} + HOO\cdot + H^+ \quad (2)$$

$$Fe^{II} + H_2O_2 \rightarrow Fe^{III} + HO\cdot + OH^- \quad (3)$$

$$HO\cdot + H_2O_2 \rightarrow HOO\cdot + H_2O \quad (4)$$

$$HOO\cdot \rightarrow H^+ + O_2^{\cdot-} \quad (5)$$

$$O_2^{\cdot-} + HO\cdot \rightarrow {}^1O_2 + OH^- \quad (6)$$

$$HOO\cdot + O_2^{\cdot-} \rightarrow {}^1O_2 + HOO^- \quad (7)$$

$$HOO\cdot + HOO\cdot \rightarrow {}^1O_2 + H_2O_2 \quad (8)$$

$${}^1O_2 + \text{organics} \rightarrow \text{intermediates} \rightarrow CO_2 + H_2O \quad (9)$$

Simultaneously, the recovered adsorption sites provide a durative supply of TC molecule for Fenton-like system. All in all, the combination of both adsorption and Fenton-

like reaction could be regarded as cleaner, greener, favored, and promising technology for removing organics from water.

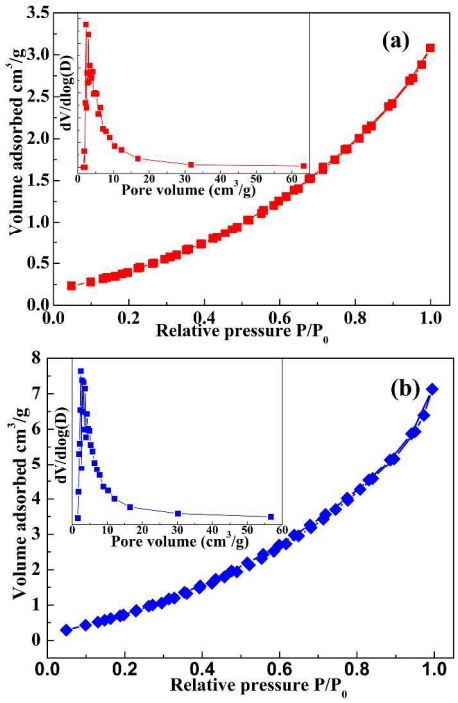

Fig.4 N_2 adsorption/desorption Isotherms and BJH pore size distributions (inset) of (a) Bacillus subtilis and (b) Fe^{2+}@B. subtilis.

Effect of H_2O_2 dosage

Hydrogen peroxide concentration is an important parameter for the degradation of the organic pollutants in the heterogeneous Fenton-like reaction system. Fig. 7a shows the removal efficiency of tetracycline hydrochloride as a function of the H_2O_2 (30%) dosage in the solution and the results showed that 2mL was the best dosage of H_2O_2 assayed when the initial concentration of TC was 30mgL^{-1} and the amount of catalyst 0.5 g L^{-1}. The reaction went more slowly when the concentration was lower (1 mL) or higher (5 mL). At low concentration, H_2O_2 cannot generate enough HO· radicals and the oxidation rate is logically slow [14, 33]. The increase of the oxidant dosage from 1 to 2 mL leads to an increase in the reaction rate, as expected, because more radicals formed. Nevertheless, for a relatively higher H_2O_2 dosage (5 mL), the performance decreases. This is because ·OH radicals efficiently react with excess hydrogen peroxide in reaction system (Eq. (4)), which contributes to the ·OH-scavenging [35]. It is noteworthy that Eq.4 shows the generation of another radical HO_2·, but its oxidation ability is significantly lower than that of the ·OH radicals, leading to negligible contribution to the organic degradation [36]. As a consequence, an optimum value of about 2mL for the hydrogen peroxide dosage was obtained when the initial concentration of the tetracycline hydrochloride was 30 mg L^{-1}.

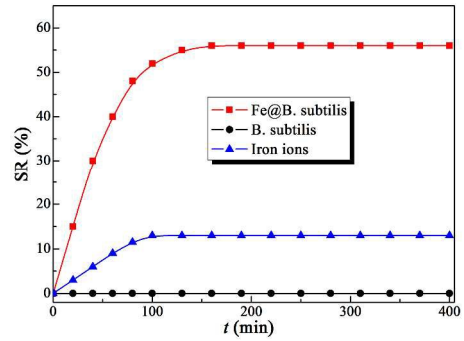

Fig. 5 Settling curves of Fe@*B. subtilis*, *B. subtilis* and iron ions;

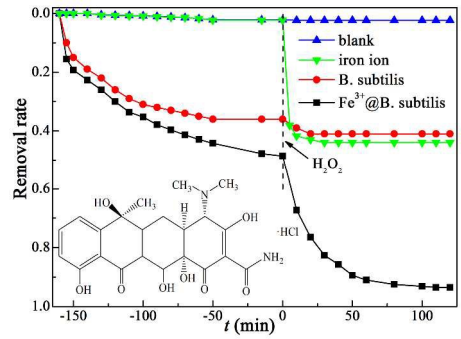

Fig.6 TC removal by self-photolysis, bare *B. subtilis*, ferric ion (0.003mM) and Fe@*B. subtilis*(0.5g/L) (inset: chemical structure of TC). Reaction conditions: initial concentration of TC, 25mg L^{-1}; H_2O_2 2mL, room temperature, agitation speed 130 rpm.

Iron leaching and stability

At the termination of each experimental run under optimum H_2O_2 concentration, the supernatant of the reaction solution was analyzed by atomic absorption spectroscopy and the equilibrium solubility of iron in the solution is about 2 mg L^{-1} which represents 2% of the total amount of iron loaded on the Fe@ *B. subtilis* catalyst (Fig.7b). Such a low extent of iron release may be regarded as the iron resistance to the leaching process [35]. Apart from the catalytic activity of the catalyst in the heterogeneous Fenton-like process, another important property is its long-term stability. To test the long-term stability of the catalyst, Fe@ *B. subtilis* was re-collected by filtration from the reaction solution, washed with distilled water and then tested again under the same reaction conditions. The results showed that the catalytic behaviour of Fe@ *B. subtilis* could be maintained in three consecutive runs without a significant drop (96.0~85%) in the degradation efficiency (Fig.7b). Besides, as the pH variation depicted in Fig. 7b, the solution showed a decrease of the initial TC aqueous solution pH (~6.0), which was normally attributed to the formation of low molecular weight organic acid [37].

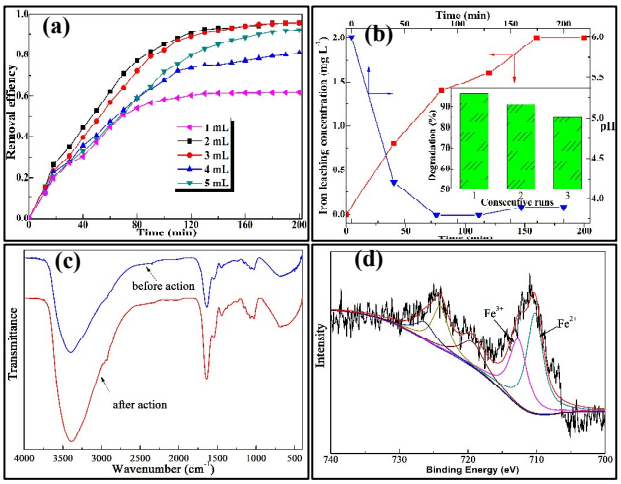

Fig.7 (a) Effect of H_2O_2 concentrations on the removal of TC. Reaction conditions: initial concentration of TC, 30mg L^{-1}; catalyst dosage 0.5 g L^{-1}, room temperature, agitation speed 130 rpm. (b) Iron leaching, stability and pH variation test. Reaction conditions: initial concentration of TC, 30mg L^{-1}; catalyst dosage 0.5 g L^{-1}, H_2O_2 addition, 2 mL; room temperature, agitation speed 130 rpm. (c) FT-IR spectra of Fe@*B. subtilis* composites before and after Fenton-like reaction; (d) XPS spectrum of iron after Fenton-like reaction.

In addition, FT-IR spectra of the catalyst before and after the three consecutive runs were recorded (Fig. 7c). It could be seen that there was no obvious change in the chemical structure of the Fe@*B. subtilis* before and after the treatment process. To investigate the structure of the catalyst after the Fenton reaction, XPS was obtained after 3 repeated reuses (Fig. 7d). This result indicates the presence of two oxidation states for the surface iron species after being used. The Fe $2p_{3/2}$ (Fe $2p_{1/2}$) spectrum was resolved into two peaks at 710.9 and 712.9 eV (724.5 and 726.9 eV), which compared well with the Fe^{2+} octahedral species and Fe^{3+} tetrahedral species [27, 33, 38]. This indicated that part of Fe^{3+} in the outermost layer of the catalyst was deoxidized into Fe^{2+} during the Fenton reaction, which was in accordance with reaction mechanism illustrated in Eq.(2).

Conclusions

For the first time, the heterogeneous catalytic oxidation of Tetracycline Hydrochloride, using an iron-impregnated *B. subtilis* as the catalyst, was investigated. EDS, EDX and XPS was evidenced that the iron in the samples was ferric ions. The as-prepared Fe@ *B. subtilis* showed excellent catalytic performance in TC degradation, and the optimal dosage of H_2O_2 was 2 mL under the reaction conditions. The Fe@ *B. subtilis* exhibited good reusability and stability because its catalytic performance could be maintained in three consecutive runs with a slight drop from 96% to 88%. The FTIR and XPS characterizations of the catalyst before and after Fenton-like reaction showed that the no structural deformation of the particles was occurred. The catalyst used has evidenced no short term decrease of activity, and was one of the first being reported for application in heterogeneous Fenton-like degradation of TC. Moreover, the low iron leaching will not lead to the iron-containing waste sludge, which might be a great progress in the industrial application.

Acknowledgements

This work was financially supported by National Natural Science Foundation of China (No.21176031), Shanxi Provincial Natural Science Foundation of China (No. 2015JM2071), the China Scholarship Council (CSC Nos. 201506560012) and Fundamental Research Funds for the Central Universities-Excellent Doctoral Dissertation Cultivation Project of Chang'an University (No.310829150004).

Notes and references

[a] College of Environmental Science and Engineering, Chang'an University, Xi'an 710054, P. R. China;
[b] Key Laboratory of Tibetan Medicine Research, Northwest Plateau Institute of Biology, Chinese Academy of Sciences, Xining, 810001, P. R. China;
Fax: +86 29 82339961;
Tel: +86 29 82339962;
E-mail: baibochina@163.com (Bai Bo)

1. M. H. Khan, H.Ba and J. Y. Jung. J. Hazard. Mater. 2010, **1**, 659.
2. W. Ben, Z. Qiang, X. Pan and M. Chen. Water Res. 2009, **17**, 4392.
3. A. K. Sarmah, M. T. Meyer and A. B. A. Boxall. Chemosphere 2006, **5**, 725.
4. X. Yu, Z. Lu, D. Wu, P. Yu, M. He, T. Chen, W. Shi, P. Huo, Y. Yan and Y. Feng. React. Kinet. Mech. Cat. 2014, **1**, 347.
5. R. Hao, X. Xiao, X. Zuo, J. Nan and W. Zhang. J. Hazard. Mater. 2012, **209**, 137.
6. Y. Chen, N. Li, Y. Zhang and L. Zhang. J. colloid Interf. Sci. 2014, **422**, 9.
7. Y. Kuang, Q. Wang, Z. Chen, M. Megharaj and R. Naidu. J. colloid Interf. Sci. 2013, **410**, 67.
8. I. Mesquita, L. C. Matos, F. Duarte, F.J. Maldonado-Hódar, A. Mendes and L. M. Madeira. J. Hazard. Mater. 2012, **237**, 30.
9. F. Duarte, F.J. Maldonado-Hódar and L.M. Madeira, Appl. Catal. B Environ. 2011, **103**, 109.
10. E. V. Kuznetsova, E. N. Savinov, L. A. Vostrikova and V.N. Parmon. Appl. Catal. B Environ. 2004, **3**, 165.
11. R. Aravindhan, N. N. Fathima, J. R. Rao and B. U. Nair. J. Hazard. Mater. 2006, **1**, 152.
12. J. Fernandez, J. Bandara, A. Lopez, P. Buffat and J. Kiwi. Langmuir 1999, **1**, 185.
13. T. Yuranova, O. Enea, E. Mielczarski E, J. Mielczarski, P. Albers and J. Kiwi. Appl. Catal. B: Environ. 2004, **1**, 3.

14. M. B. Kasiri, H. Aleboyeh and A. Aleboyeh. Appl. Catal. B: Environ. 2008, **1**, 9.
15. N. K. Daud, M. A. Ahmad and B. H. Hameed. Chem. Eng. J. 2010, **1**, 111.
16. I. Fatimah, I. Sumarlan and T. Alawiyah. Int. J. Chem. Eng. 2015, 2015.
17. C. Ya, D. Feng, Y. Jiang, X. An, L. Ye, W. Guan and B. Bai. Cata. Lett. 2015, **6**, 1301.
18. Z. Filip, S. Herrmann, J. Kubat. Microbiol. Res. 2004, **3**, 257.
19. A. Ayla, A. Çavuş, Y. Bulut, Z. Baysal and C. Aytekin. Desalin. Water Treat. 2013, **51**, 7596.
20. K. Ashtari, J. Fasihi, N. Mollania and K. Khajeh. Mater. Res. Bull. 2014, **50**, 348.
21. T. J. Beveridge and R. G. Murray. J. Bacteriol. 1980, **2**, 876.
22. Y. Tian, C. Ji, M. Zhao, M. Xu, Y. Zhang and R. Wang. Chem. Eng. J. 2010, **2**, 474.
23. C. Zhu, S. Guo, Y. Fang and S. Dong. ACS nano. 2010, **4**, 242.
24. M. Acik, C. Mattevi, C. Gong, G. Lee, K. Cho, M. Chhowalla and Y. J. Chabal. ACS nano. 2010, **10**, 5861.
25. M. Song and J. Xu. Electroanal. 2013, **2**, 523.
26. N. A. Zubir, C. Yacou, J. Motuzas, X. Zhang and J. C. Diniz da Costa. Sci. Rep-UK, 2014, **4**, 4594.
27. T. Yamashita and P. Hayes. Applied Surf. Sci. 2008, 8, 2441.
28. B. Sun, W. Zhao, Y. Xiong, Y. Lin and P. Chen. Metall. Mater. Trans. A 2014, **11**, 5245.
29. S. Zhong, M. Wang, L. Wang, Y. Li, H. M. Noh and J. H. Jeong, Cryst. Eng. Comm., 2014, **16**, 231.
30. A. Silvestre-Albero, J. Silvestre-Albero, M. Martínez-Escandell and F. Rodríguez-Reinoso, Ind. Eng. Chem. Res., 2014, **53**, 15398.
31. N. K. Daud and B. H. Hameed. J. Hazard. Mater. 2010, **1**, 1118.
32. Z.M. Cui, Z. Chen, C. Y. Cao, L. Jiang and W.G. Song, Chem. Commun. 2013, **49**, 2332.
33. X. Li, J. Liu, A.I. Rykov, H. Han, C. Jin, X. Liu and J. Wang, Appl. Catal. B: Environ.2015, **179**, 196.
34. J.V. Coelho, M.S. Guedes, R.G. Prado, J. Tronto, J.D. Ardisson, M.C. Pereira and L.C.A. Oliveira, Appl. Catal. B: Environ. 2014, **144**, 792.
35. M. Bayat, M. Sohrabi and S. J. Royaee. J. Ind. Eng. Chem. 2012, **3**, 957.
36. R.J. Bigda, Chem. Eng. Prog. 1995, **91**, 62.
37. Y. Yan, S. Jiang, H. Zhang. Sep. Purif. Technol. 2014,133, 365.
38. C. Bao, H. Zhang, L. Zhou, Y. Shao and J. Ma, Q. Wu. RSC Adv. 2015, **88**, 72423.

Graphical Abstract

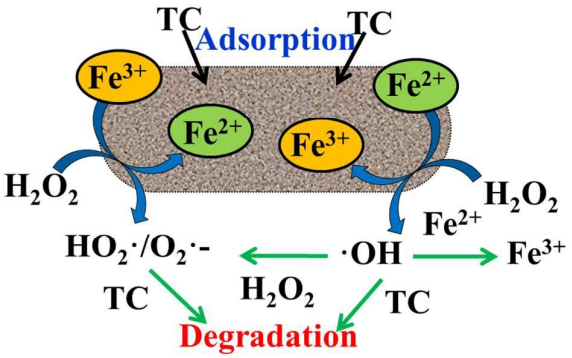

In this work, a novel heterogeneous catalyst Fe@*Bacillus subtilis* was firstly fabricated via a simple impregnation method and its catalytic efficiency was examined for removal of Tetracycline Hydrochloride.